

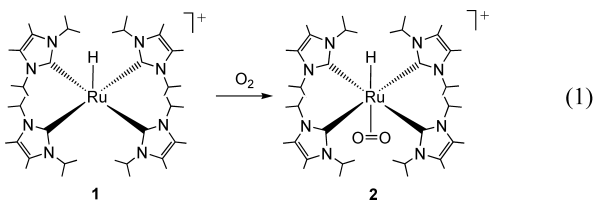
Formation of $[\text{Ru}(\text{NHC})_4(\eta^2\text{-O}_2)\text{H}]^+$: An Unusual, High Frequency Hydride Chemical Shift and Facile, Reversible Coordination of O_2

L. Jonas L. Häller,[†] Elena Mas-Marzá,[‡] Aitor Moreno,[§] John P. Lowe,[‡] Stuart A. Macgregor,^{*,†} Mary F. Mahon,[‡] Paul S. Pregosin,[§] and Michael K. Whittlesey^{*,‡}

School of Engineering and Physical Sciences, Heriot-Watt University, Edinburgh, EH14 4AS, U.K., Department of Chemistry, University of Bath, Claverton Down, Bath, BA2 7AY, U.K., and Laboratorium für Anorganische Chemie, ETHZ HCI, Höggerberg, CH-8093 Zürich, Switzerland

Received May 14, 2009; E-mail: s.a.macgregor@hw.ac.uk; m.k.whittlesey@bath.ac.uk

The coordination and activation of dioxygen by transition metal complexes continues to be the focus of considerable interest in attempts to develop new, atom economical oxidation catalysts for organic synthesis.¹ N-heterocyclic carbenes (NHCs) are very promising ligands in this field due to their ability to support high-oxidation state metal complexes with strong $\text{M}-\text{C}_{\text{NHC}}$ bonds which should enhance stability under oxidizing conditions.² However, the rational design of any new NHC based catalysts first requires a fundamental understanding of how O_2 interacts with different $\text{M}-\text{NHC}$ fragments and the impact of oxygen coordination/activation on their chemical and structural properties. We now report an experimental and computational study on the reaction of the tetrakis-carbene ruthenium cation $[\text{Ru}(\text{IPr}_2\text{Me}_2)_4\text{H}]^+$ (**1**, $\text{IPr}_2\text{Me}_2 = 1,3\text{-diisopropyl-4,5-dimethylimidazol-2-ylidene}$) with oxygen which affords the $\eta^2\text{-O}_2$ hydride species $[\text{Ru}(\text{IPr}_2\text{Me}_2)_4(\eta^2\text{-O}_2)\text{H}]^+$ (**2**, eq 1). **2** displays (i) a very facile, reversible O_2 coordination and (ii) an unexpectedly positive hydride chemical shift, and both these features can be predicted and explained by density functional theory (DFT) calculations.



Addition of 1 atm of O_2 at room temperature to $\text{C}_5\text{D}_5\text{N}$ or CD_2Cl_2 solutions of $[\text{1}[\text{BAR}_4^{\text{F}}]]$ ($\text{BAR}_4^{\text{F}} = \text{B}\{(3,5\text{-CF}_3)_2\text{C}_6\text{H}_3\}_4$) resulted in an instantaneous color change from purple to pink with the formation of a single new product, $[\text{2}[\text{BAR}_4^{\text{F}}]]$. While those regions of the ^1H NMR spectrum associated with the NHC were very similar for both colored solutions (**1** and **2** displayed nonequivalent ^iPr and backbone methyl ^1H resonances due to the perpendicular arrangement of the imidazol-2-ylidene rings with respect to the plane defined by the four carbene C-atoms and the metal center), the addition of O_2 led to the complete disappearance of the very low frequency hydride resonance of **1** at $\delta -41.2$ and formation of a new resonance of integral one at $\delta +4.8$. While the high frequency of this signal suggested initially that **2** could be the hydroperoxy cation, $[\text{Ru}(\text{IPr}_2\text{Me}_2)_4(\text{OOH})]^+$,³ we have been able to exclude this possibility by a combination of structural, spectroscopic, and computational studies. The molecular structure of **2** (Figure 1) clearly shows a side-on bound O_2 molecule, with $\text{O}-\text{O}$ and $\text{Ru}-\text{O}$

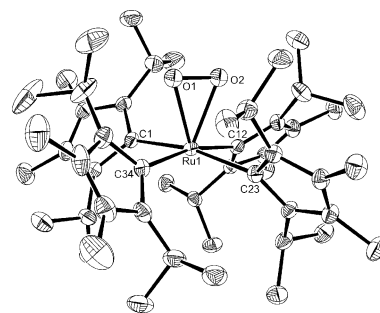


Figure 1. Molecular structure of **2**. Thermal ellipsoids are shown at the 30% probability level, and all hydrogen atoms are omitted for clarity. Selected bond lengths (Å): $\text{Ru}(1)-\text{O}(1)$ 2.088(3), $\text{Ru}(1)-\text{O}(2)$ 2.087(3), $\text{Ru}(1)-\text{C}(1)$ 2.171(4), $\text{Ru}(1)-\text{C}(12)$ 2.176(4), $\text{Ru}(1)-\text{C}(23)$ 2.162(4), $\text{Ru}(1)-\text{C}(34)$ 2.138(4), $\text{O}(1)-\text{O}(2)$ 1.354(5).

distances of 1.354(5) and 2.088(3)/2.087(3) Å.⁴ This immediately excludes an $\eta^1\text{-OOH}$ structure, although the intrinsic difficulty in structurally locating hydrogen atoms meant an $\eta^2\text{-OOH}$ structure could not be ruled out. Firm evidence for the formulation of **2** as an η^2 -dioxygen hydride complex came from the IR spectrum, which displayed a clear $\text{Ru}-\text{H}$ stretch at 1992 cm^{-1} (c.f. 2054 cm^{-1} for **1**)⁵ along with a lower frequency band at 1047 cm^{-1} assigned to the $\text{O}-\text{O}$ stretch ($^{18}\text{O}_2$ labeling shifted this to 992 cm^{-1} , close to the calculated value of 987 cm^{-1}). The $T_1(\text{min})$ value of 124 ms (400 MHz, 216 K) measured for the resonance at $\delta +4.8$ was comparable to the values found for the hydride signals of **1** ($\delta -41.2$: 98 ms, 400 MHz, 204 K) and $[\text{Ru}(\text{IPr}_2\text{Me}_2)_4(\text{CO})\text{H}][\text{BAR}_4^{\text{F}}]$ (**3** [$\text{BAR}_4^{\text{F}}]$) ($\delta -3.1$: 137 ms, 400 MHz, 222 K). Moreover, the J -resolved $^1\text{H}-^{13}\text{C}$ HMBC spectrum of **2** (220 K) revealed a coupling constant of 5.2 Hz between the $\delta +4.8$ signal and the ^{13}C carbene resonance at $\delta 176$, a value comparable to those recorded in **1** (5.0 Hz) and **3** (4.8 Hz). Finally, $^1\text{H}-^1\text{H}$ NOESY data revealed a strong contact between the hydride signal at $\delta +4.8$ and one of the two ^iPr methine CH resonances.

DFT calculations⁶ on **2** confirmed the *trans*- $\text{H}-\text{Ru}(\eta^2\text{-O}_2)$ structure with no minimum corresponding to the alternative five-coordinate $\eta^2\text{-OOH}$ form being located.⁷ The details of the computed structure also agree well with experiment ($\text{Ru}-\text{O}(\text{av}) = 2.11\text{ Å}$, $\text{O}-\text{O} = 1.37\text{ Å}$, $\text{Ru}-\text{C}(\text{av}) = 2.19\text{ Å}$, $\text{Ru}-\text{H} = 1.61\text{ Å}$); **2** is therefore a rare example of a dioxygen adduct with an unusually short $\text{O}-\text{O}$ distance.^{4,8} Quantitative formation of **2** was shown by ^1H NMR spectroscopy to occur upon addition of O_2 to **1** at temperatures as low as 193 K. Moreover, the coordinated O_2 ligand proved to be only weakly bound and, in stark contrast to other $\text{M}(\eta^2\text{-O}_2)$ species,⁹ could be removed by simple freeze-pump-thaw degassing of solutions of **2**. The reversible coordination of O_2 even took place in the solid state; exposing solid **1** to 1 atm of O_2 at 298

[†] Heriot-Watt University.

[‡] University of Bath.

[§] ETHZ.

K led to the same purple to pink color change associated with formation of **2**, while application of a vacuum regenerated purple **1** (IR spectroscopy confirmed the transformation). This remarkably reversible oxygen coordination prompted us to compute the energy profile for $^3\text{O}_2$ addition to **1** (Figure 2). This is initiated by the barrierless formation of triplet *trans*-[Ru($\text{I}^{\text{Pr}}_2\text{Me}_2$) $_4(\eta^1\text{-O}_2)\text{H}]^+$ (**$^3\mathbf{2}$** , $E = +0.5$ kcal/mol) with a Ru–O–O angle (θ) of 161.5° .¹⁰ Reducing θ in **$^3\mathbf{2}$** to give singlet **2** (denoted hereafter **$^1\mathbf{2}$**) revealed the presence of a second triplet state, **$^3\mathbf{2b}$** ($E = +7.0$ kcal/mol, $\theta = 109.9^\circ$). **$^3\mathbf{2b}$** was shown to link **$^3\mathbf{2}$** and **$^1\mathbf{2}$** via crossover points at $\theta \approx 125^\circ$ and 90° , respectively. For the latter a triplet-singlet minimum energy crossing point (MECP) was located¹¹ ($\theta = 91.1^\circ$, $E = 12.0$ kcal/mol), and this represents the barrier to interconversion between **$^3\mathbf{2}$** and **$^1\mathbf{2}$** . Figure 2 also maps how charge density transfers from Ru to O_2 in forming **$^1\mathbf{2}$** . The most significant change occurs in forming **$^3\mathbf{2}$** , and this, along with computed spin densities,¹² suggests this species (and **$^3\mathbf{2b}$**) are correctly formulated as Ru^{III}-superoxo complexes. Formation of **$^1\mathbf{2}$** then sees a further partial reduction of the $\{\text{O}_2\}$ moiety.

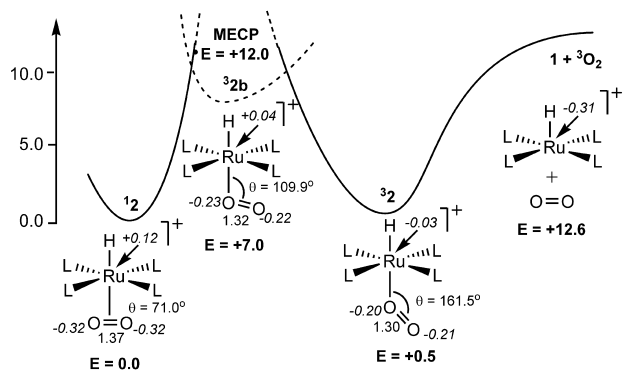


Figure 2. Computed energy profile (kcal/mol) for the addition of $^3\text{O}_2$ to **1** with potential energy curves for variation of the Ru–O–O angle, θ , in **$^3\mathbf{2}$** , **$^3\mathbf{2b}$** , and **$^1\mathbf{2}$** ($\text{L} = \text{I}^{\text{Pr}}_2\text{Me}_2$). Also shown are values for θ and O–O distances (\AA , degrees, plain text) and natural atomic charges at Ru and O (italics).

Overall, the O_2 addition profile for **1** is similar to that described for PdL_2/O_2 systems,¹³ except for the involvement of the second triplet state (**$^3\mathbf{2b}$**) in the present case. The highly reversible nature of O_2 binding to **1** is reflected in the Ru– O_2 binding energy which was computed to be only 12.6 kcal/mol, while the computed free energy change is only 3.5 kcal/mol (in favor of $^3\text{O}_2 + \mathbf{1}$). This low binding energy may reflect the less electron-releasing nature of square-pyramidal d^6 $\{\text{ML}_5\}$ fragments over C_{2v} , d^{10} $\{\text{ML}_2\}$ species; however, we believe the steric bulk of the $\text{I}^{\text{Pr}}_2\text{Me}_2$ ligand is a key factor here: with $[\text{Ru}(\text{IME}_4)_4(\eta^2\text{-O}_2)\text{H}]$ ($\text{IME}_4 = 1,3,4,5\text{-tetramethylimidazol-2-ylidene}$) the computed O_2 binding energy increases to 27.4 kcal/mol, while for $[\text{Ru}(\text{I}^{\text{Pr}}_2\text{P}(\text{CH}_2)_2\text{P}^{\text{Pr}}_2)(\eta^2\text{-O}_2)\text{H}]^+$ a value of 24.1 kcal/mol is obtained.⁴

DFT calculations were also performed to probe the unusual positive chemical shift associated with the hydride ligand of **2**,^{14,15} which contrasts markedly with the more standard negative chemical shifts reported for the phosphine analogues $[\text{Ru}(\text{P}(\text{P})_2)(\eta^2\text{-O}_2)\text{H}]^+$ ($\text{P}(\text{P}) = \text{R}_2\text{P}(\text{CH}_2)_2\text{PR}_2$, $\text{R} = \text{I}^{\text{Pr}}$, Cy : $\delta = -5.9$).⁴ Calculations on both **$^1\mathbf{2}$** and $[\text{Ru}(\text{I}^{\text{Pr}}_2\text{P}(\text{CH}_2)_2\text{P}^{\text{Pr}}_2)(\eta^2\text{-O}_2)\text{H}]^+$ satisfactorily reproduce these differences with $\delta_{\text{calc}} = +5.3$ and -4.5 , respectively. Partitioning of the various components of these computed chemical shifts indicate that the diamagnetic and spin-orbit terms are approximately constant in the NHC and P–P systems. The major difference arises from the paramagnetic term that yields a high

frequency 5.3 ppm contribution in **2** but a low frequency 5.6 ppm in $[\text{Ru}(\text{I}^{\text{Pr}}_2\text{P}(\text{CH}_2)_2\text{P}^{\text{Pr}}_2)(\eta^2\text{-O}_2)\text{H}]^+$.

In summary, we have shown that the NHC complex **1** reacts with O_2 to afford the η^2 -dioxygen hydride complex **2** which displays unusual and very different chemical and spectroscopic properties to the related phosphine derivatives. Efforts to alter the coordinating ability of derivatives of **1** through manipulation of sterics by changing the N-substituents on the NHC ligands are currently underway.

Acknowledgment. We acknowledge support from the EPSRC (L.J.L.H.), the Spanish Ministerio de Ciencia e Innovación (E.M.M.), and the Swiss National Science Foundation. We thank Johnson Matthey plc for the loan of hydrated ruthenium chloride and Prof. Jeremy Harvey (University of Bristol) for use of the MECP location program.

Supporting Information Available: Spectroscopic data for **1–3**, X-ray structures of **1** and **3**, X-ray files (CIF format) for **1–3** (CCDC 713540–713542). Computed Cartesian coordinates and energies; full refs 6 and 14. This material is available free of charge via the Internet at <http://pubs.acs.org>.

References

- (1) (a) Klotz, I. M.; Kurtz, D. M. *Chem. Rev.* **1994**, *94*, 567–568. (b) Punniyamurthy, T.; Velusamy, S.; Iqbal, J. *Chem. Rev.* **2005**, *105*, 2329–2364. (c) Cornell, C. N.; Sigman, M. S. In *Activation of Small Molecules*; Tolman, W. B., Ed.; Wiley-VCH: Weinheim, 2006; pp 159–186.
- (2) Rogers, M. M.; Sigman, M. S. *Top. Organomet. Chem.* **2007**, *21*, 21–46.
- (3) (a) Wick, D. D.; Goldberg, K. I. *J. Am. Chem. Soc.* **1999**, *121*, 11900–11901. (b) Konnick, M. M.; Guzei, I. A.; Stahl, S. S. *J. Am. Chem. Soc.* **2004**, *126*, 10212–10213.
- (4) This is comparable to the O–O distance of 1.360(10) \AA reported for $[\text{Ru}(\text{d}^{\text{ppe}})_2(\eta^2\text{-O}_2)\text{H}]^+$ ($\text{d}^{\text{ppe}} = \text{I}^{\text{Pr}}_2\text{P}(\text{CH}_2)_2\text{P}^{\text{Pr}}_2$). (a) Jiménez-Tenorio, M.; Puerta, M. C.; Valerga, P. *J. Am. Chem. Soc.* **1993**, *115*, 9794–9795. (b) Jiménez-Tenorio, M.; Puerta, M. C.; Valerga, P. *Inorg. Chem.* **1994**, *33*, 3515–3520.
- (5) Failure to prepare **1-D** (treatment of **1** with D_2O did not exchange Ru–H for Ru–D, while reaction of $\text{Ru}(\text{P}(\text{Ph})_3)_3\text{DCl}$ with $\text{I}^{\text{Pr}}_2\text{Me}_2$ led to room temperature H/D exchange into the $\text{I}^{\text{Pr}}\text{-Me}$ groups) precluded us from recording the IR spectrum of $[\text{Ru}(\text{I}^{\text{Pr}}_2\text{Me}_2)_4(\eta^2\text{-O}_2)\text{D}]^+$ (**2-D**).
- (6) Frisch, M. et al. *Gaussian 03*, revision D.01; Gaussian, Inc.: Pittsburgh, PA, 2001. The BP86 functional was used with SDD RECPs and basis sets on Ru and P (with d-orbital polarization on the latter) and 6-31G** basis sets on all other atoms. See Supporting Information for full details.
- (7) Attempted optimization led instead to an η^1 -OOH geometry which was 1.4 kcal/mol higher in energy than the *trans*-H-Ru- $(\eta^2\text{-O}_2)$ form.
- (8) (a) Praetorius, J. M.; Allen, D. P.; Wang, R.; Webb, J. D.; Grein, F.; Kennepohl, P.; Crudden, C. M. *J. Am. Chem. Soc.* **2008**, *130*, 3724–3725. (b) Verat, A. Y.; Fan, H. J.; Pink, M.; Chen, Y. S.; Caulton, K. G. *Chem.–Eur. J.* **2008**, *14*, 7680–7686. (c) Frech, C. M.; Shimon, L. J. W.; Milstein, D. *Helv. Chim. Acta* **2006**, *89*, 1730–1739.
- (9) (a) Reference 4. (b) Mezzetti, A.; Zangrando, E.; Del Zotto, A.; Rigo, P. *J. Chem. Soc., Chem. Commun.* **1994**, 1597–1598. (c) References 8b and 8c.
- (10) Calculation of the singlet-triplet gap ($\Delta E^{\text{S-T}}$) with a range of functionals and basis sets indicate that **$^1\mathbf{2}$** and **$^3\mathbf{2}$** remain close in energy (e.g., $\Delta E^{\text{S-T}}$: B3LYP = -0.3 kcal/mol; TPSSH = $+2.4$ kcal/mol).
- (11) Harvey, J. N.; Aschi, M.; Schwarz, H.; Koch, W. *Theor. Chem. Acc.* **1998**, *99*, 95–99.
- (12) Computed spin densities: **$^3\mathbf{2}$** : +0.59 (Ru), +1.38 (O_2); **$^3\mathbf{2b}$** : +0.62 (Ru), +1.26 (O_2).
- (13) Popp, B. V.; Wendlandt, J. E.; Landis, C. R.; Stahl, S. S. *Angew. Chem., Int. Ed.* **2007**, *46*, 601–604. (b) Landis, C. R.; Morales, C. M.; Stahl, S. S. *J. Am. Chem. Soc.* **2004**, *126*, 16302–16303.
- (14) ADF 2007.01, SCM, Theoretical Chemistry, Vrije Universiteit, Amsterdam, The Netherlands (<http://www.scm.com>). Calculations on the Gaussian 03 optimized structures used the BP86 functional and TZ2P all electron basis sets and included corrections for scalar relativistic and spin-orbit coupling effects through the ZORA approach. NMR parameters^{14b} included relativistic effects via the mass-velocity, Darwin, and spin-Zeeman terms. (b) Schreckenbach, G.; Ziegler, T. *J. Phys. Chem.* **1995**, *99*, 606–611. See Supporting Information for full details.
- (15) High frequency chemical shifts are known for a number of early transition metal hydride complexes. (a) Chisholm, M. H.; Eichhorn, B. W.; Huffmann, J. C. *J. Chem. Soc., Chem. Commun.* **1985**, 861–862. (b) Caffyn, A. J. M.; Feng, S. G.; Dierdorf, A.; Gamble, A. S.; Eldredge, P. A.; Vossen, P. R.; White, P. S.; Templeton, J. L. *Organometallics* **1991**, *10*, 2842–2848. (c) Figueroa, J. S.; Cummins, C. C. *J. Am. Chem. Soc.* **2003**, *125*, 4020–4021.

JA9039345